Petre Flaviu Gostin, Dimitri Eigel, Daniel Grell, Jürgen Eckert, Eberhard Kerscher, Annett Gebert

Comparing the pitting corrosion behavior of prominent Zr-based bulk metallic glasses

Erstveröffentlichung in / First published in:

Journal of materials research. 2015, 30 (2), S. 233-241 [Zugriff am: 13.03.2020]. Cambridge University Press. ISSN 2044-5326.

DOI: https://doi.org/10.1557/jmr.2014.371

Comparing the pitting corrosion behavior of prominent Zr-based bulk metallic glasses

Petre Flaviu Gostin[a)]
Leibniz-Institute for Solid State and Materials Research IFW Dresden, Dresden D-01171, Germany

Dimitri Eigel
Leibniz-Institute for Solid State and Materials Research IFW Dresden, Dresden D-01171, Germany; and Department of Chemistry and Food Chemistry, Faculty of Science, TU Dresden, Dresden D-01069, Germany

Daniel Grell
Materials Testing, University of Kaiserslautern, Gottlieb-Daimler-Straße, Kaiserslautern D-67663, Germany

Jürgen Eckert[b)]
Leibniz-Institute for Solid State and Materials Research IFW Dresden, Dresden D-01171, Germany; and Institute of Materials Science, Faculty of Mechanical Science and Engineering, TU Dresden, Dresden D-01062, Germany

Eberhard Kerscher
Materials Testing, University of Kaiserslautern, Gottlieb-Daimler-Straße, Kaiserslautern D-67663, Germany

Annett Gebert
Leibniz-Institute for Solid State and Materials Research IFW Dresden, Dresden D-01171, Germany

(Received 20 August 2014; accepted 11 November 2014)

Five well-known Zr-based alloys of the systems Zr–Cu–Al–(Ni–Nb, Ni–Ti, Ag) (Cu = 15.4–36 at.%) with the highest glass-forming ability were comparatively analyzed regarding their pitting corrosion resistance and repassivation ability in a chloride-containing solution. Potentiodynamic polarization measurements were conducted in the neutral 0.01 M Na_2SO_4 + 0.1 M NaCl electrolyte and local corrosion damages were subsequently investigated with high resolution scanning electron microscopy (HR-SEM) coupled with energy dispersive x-ray spectroscopy (EDX). Both pitting and repassivation potential correlate with the Cu concentration, i.e., those potentials decrease with increasing Cu content. Pit morphology is not composition dependent: while initially hemispherical pits then develop an irregular shape and a porous rim. Corrosion products are rich in Cu, O, and often Cl species. A combination of low Cu and high Nb or Ti contents is most beneficial for a high pitting resistance of Zr-based bulk metallic glasses. The bulk glassy $Zr_{57}Cu_{15.4}Al_{10}Ni_{12.6}Nb_5$ (Vit 106) and $Zr_{52.5}Cu_{17.9}Al_{10}Ni_{14.6}Ti_5$ (Vit 105) alloys exhibit the highest pitting resistance.

I. INTRODUCTION

Among the various families of bulk metallic glasses (BMGs), the Zr-based alloys are until today most actively studied. The strong interest in Zr-based BMGs is due to their high glass-forming ability and excellent mechanical properties such as very high strength and large elastic deformation capability at room temperature. These qualities render them attractive for various applications, e.g., sporting goods, springs, or electronic casings.[1] For most of those applications, a high corrosion resistance in various environments is mandatory for a long lifetime of a part made from a BMG. Fabrication of bulk parts (thickness >1 mm) requires alloys with the highest glass-forming ability. Therefore, this study focuses on a comparative corrosion analysis of different Zr–Cu-based alloys, which are well known as excellent bulk glass formers.

The corrosion behavior of Zr-based bulk and non-BMGs has been the subject of a number of fundamental studies. They exhibit excellent passivation ability in halide-free electrolytes owing to easy formation of passive films rich in Zr oxides.[2–6] At the same time, however, they are quite susceptible to pitting corrosion in halide-containing environments.[2,4,5,7–11] Alloying elements may have a significant influence on both their passivation ability and their pitting susceptibility.[6,7,12–16] A clear understanding of those alloying effects is necessary for the design of new Zr-based BMGs with improved pitting corrosion resistance.

Most of the Zr-based BMGs are composed of a combination of valve metals, e.g., Zr, Al, Nb, or Ti,

[a)]Address all correspondence to this author.
e-mail: f.p.gostin@ifw-dresden.de
[b)]This author was an editor of this journal during the review and decision stage. For the *JMR* policy on review and publication of manuscripts authored by editors, please refer to http://www.mrs.org/jmr-editor-manuscripts/.
DOI: 10.1557/jmr.2014.371

with late transition metals, e.g., Cu, Ni, Ag, Fe, or Co, in well-defined concentration ratios. According to surface analytical studies, native and anodic passive films on Zr-based BMGs are very thin barrier-type films consisting mainly of Zr oxides. Other valve metals, like Nb and Ti, are also incorporated into the passive film[4,17–21] and are assumed to improve film properties.[13,22] As a result, the partial replacement of Zr with Nb or Ti in Zr-based metallic glasses yields an increase of the pitting potential.[12,14,23,24] On the contrary, late transition metals, e.g., Cu or Ni, are depleted in the passive film and instead tend to accumulate at the metal/film interface in the metallic state.[4,17,18,21] Moreover, Cu is considered to play a central role in the pit growth mechanism of Zr–Cu-based metallic glasses. According to a frequently proposed mechanism, the initial breakdown of the passive film occurs at weak points of the underlying metallic glass, e.g., at structural defects or at mechanically induced defects.[25] During pit growth, the local selective dissolution of Zr and other valve metal components leaves the surface locally rich in Cu species, which then react with chloride to form CuCl. CuCl in turn undergoes hydrolysis to form Cu_2O, which is deposited within the pitted region.[4,10,19,21,26–28] Consequently, it may be expected that the Cu content in Zr–Cu-based BMGs determines their pitting resistance. However, no systematic studies in this regard have been carried out so far. A major difficulty for such a study is the compositional limitation due to glass formation considerations: for a known BMG composition, it is not possible to vary the Cu content systematically and significantly without reduction of the glass-forming ability, which is related with partial crystallization upon solidification.

The objective of the present study is to compare the pitting resistance and repassivation ability of prominent Zr–Cu-based BMGs of the systems Zr–Cu–Al–(Ni–Nb, Ni–Ti, Ag) (Cu = 15.4–36 at.%). For that, the anodic polarization behavior of five BMGs, i.e., $Zr_{57}Cu_{15.4}Al_{10}Ni_{12.6}Nb_5$ (Vit 106), $Zr_{52.5}Cu_{17.9}Al_{10}Ni_{14.6}Ti_5$ (Vit 105), $Zr_{59}Cu_{20}Al_{10}Ni_8Ti_3$, $Zr_{55}Cu_{30}Al_{10}Ni_5$, and $Zr_{48}Cu_{36}Al_8Ag_8$, was studied in a selected chloride-containing electrolyte. These distinct alloy compositions were determined as being the ones at which in a specific multicomponent system the maximum glass-forming ability and therefore, the best casting-ability up to the maximum critical diameters was achieved.[1,29] Cu is in all cases the second main element and varied in this study between 15.4 and 36 at.%. The third element in these alloys is Al and its content varied in a narrow range of 8–10 at.%. Four of the alloys contain Ni in the range of 5–12.6 at.%, while one of the alloys has no Ni and instead has 8 at.% Ag. The first three alloys contain up to 5 at.% Nb or Ti, which are known to typically have a beneficial effect for pitting resistance.

Moreover, the present research focuses on analyses of crack initiation and propagation in BMGs, which determine fracture toughness and fatigue resistance. The environmental conditions appear to be of crucial importance for those phenomena.[30,31] First studies on stress corrosion cracking and fatigue corrosion phenomena of Zr-based BMGs[32,33] revealed the critical effect of NaCl solution media on enhancing the crack growth rate and reducing the fatigue endurance limit. This implies that the above-described chloride-induced local corrosion processes dominated by Cu reactions also control those stress-corrosion degradation processes. To analyze this in more detail, for selected alloy compositions, a reliable set of characteristic electrochemical corrosion parameters is needed and can be derived from the results of the present study.

II. EXPERIMENTAL

Five Zr–Cu-based BMGs with Cu concentration varying between 15.4 and 36 at.% were selected for this study. Their nominal compositions (in at.%) are: $Zr_{57}Cu_{15.4}Al_{10}Ni_{12.6}Nb_5$ (Vit 106), $Zr_{52.5}Cu_{17.9}Al_{10}Ni_{14.6}Ti_5$ (Vit 105), $Zr_{59}Cu_{20}Al_{10}Ni_8Ti_3$, $Zr_{55}Cu_{30}Al_{10}Ni_5$, and $Zr_{48}Cu_{36}Al_8Ag_8$. Ingots of each composition were prepared from a mixture of pure elements (purity 99.9% or higher) by arc melting under Ar atmosphere. The weight of ingots was 50 g and had a roughly spherical cap shape with a diameter of approximately 35 mm. To ensure a homogeneous chemical composition, the ingots were re-melted at least three times. To verify their homogeneity, chemical analysis of the ingots at three different random locations was done with inductively coupled plasma optical emission spectrometry (ICP-OES). Exemplary results for the $Zr_{59}Cu_{20}Al_{10}Ni_8Ti_3$ alloy are shown in Table I, which indicates a high level of homogeneity. Similar results were obtained for the other alloys. The oxygen concentration in the ingots was determined by carrier gas hot extraction and was found to be in the interval 0.005–0.019 wt%.

TABLE I. The chemical composition of a $Zr_{59}Cu_{20}Al_{10}Ni_8Ti_3$ alloy ingot determined at three random locations in the ingot confirming a high level of compositional homogeneity. The concentration of metallic elements was measured by ICP-OES. Each given value represents the mean of four individual measurements of the same specimen (corresponding to one location). Values in brackets represent standard deviation.

	Concentration of analyzed elements, wt%					
	Zr	Cu	Al	Ni	Ti	Sum
Location A	71.10 (0.35)	16.79 (0.10)	3.57 (0.01)	6.21 (0.04)	1.84 (0.01)	...
Location B	71.58 (0.33)	16.98 (0.04)	3.59 (0.01)	6.27 (0.01)	1.85 (0.01)	...
Location C	71.41 (0.28)	16.93 (0.03)	3.59 (0.01)	6.26 (0.01)	1.85 (0.01)	...
Mean value	71.36 (0.36)	16.90 (0.10)	3.58 (0.01)	6.25 (0.03)	1.85 (0.01)	99.94
Nominal	71.42	16.87	3.58	6.23	1.91	...

From those ingots, rods with a diameter of 2 mm and a length of 75 mm were obtained by suction casting in a water-cooled Cu mold. The rods were sectioned into several slices, which were used for subsequent investigations. X-ray diffraction (XRD) and differential scanning calorimetry (DSC) analyses confirmed their fully glassy nature (not shown here). The XRD and DSC analyses were performed at three different locations along the rod (close to the ends and in the middle) and yielded very similar results indicating a high level of homogeneity also for the rods.

For the electrochemical tests, the 15 mm long specimens of each alloy were taken from the middle region of rods and were electrically connected to a steel wire and embedded in epoxy resin. This way, only the cross-section is exposed to the environment. These specimens were then subjected to conventional metallographic procedures. Previous work demonstrated that the anodic response of Zr–Cu-based BMGs can be significantly influenced by their surface finishing state.[34] In particular, fine-polishing procedures with nanoparticle suspensions can lead to Cu enrichment at the surface. Therefore, in the present work, prior to the polarization measurements, the cross-section of the samples was prepared only by grinding using SiC abrasive paper from P360 to P4000. Repeated electrochemical tests were performed on the same embedded specimen (after re-grinding) to minimize possible effects due to the cooling rate gradient along the rod (the cooling rate at the bottom side is higher than at the top side).

The polarization tests were carried out with a Solartron SI1287 electrochemical interface and a standard three-electrode cell with a saturated calomel electrode (SCE, $E = 0.241$ V versus SHE) as the reference electrode and a Pt net as the counter electrode. All the tests were carried out in a 0.01 M Na_2SO_4 + 0.1 M NaCl solution under ambient atmosphere (without purging). Prior to immersion in the electrolyte, the ground samples were exposed to air with a relative humidity of approximately 30% at room temperature for 20 h to ensure a reproducible surface state.[34,35] Before the start of the dynamic polarization tests, the samples were maintained at open circuit conditions for 30 min, while their open circuit potential (OCP) was monitored. To study the pitting and repassivation behavior, the samples were slowly anodically polarized (0.5 mV s^{-1}) to beyond the pitting potential, and when the measured current density reached a defined value of 1 mA cm^{-2}, the polarization direction was reversed and the measurement was stopped at −0.5 V versus OCP. Each experiment was repeated at least five times. After selected polarization tests, the sample cross-sections were examined by scanning electron microscopy (SEM) and energy dispersive x-ray spectroscopy (EDX).

III. RESULTS

A. Pitting susceptibility and repassivation ability

To study the susceptibility to pitting corrosion and the repassivation ability of the different Zr–Cu-based bulk glassy alloys, potentiodynamic anodic polarization experiments were carried out in a chloride-containing electrolyte, i.e., 0.01 M Na_2SO_4 + 0.1 M NaCl. The potential was swept in the positive direction until stable pit growth was clearly established (per definition: when the current density reached a value of 1 mA cm^{-2}), and then swept backwards. Ranking of the pitting susceptibility of the investigated alloys was done according to their pitting potential, E_P, and their repassivation potential, E_R, which were determined from the polarization curves. E_P, the potential at which stable pit growth commences, is clearly indicated by a sharp increase in the current density from the passive current density level during polarization in the positive direction. However, the determination of E_R, defined as the potential at which pits repassivate during the backward scan, is not as straightforward and various methods have been proposed.[36] Here, E_R was conventionally taken as the potential at which the measured current density decreases abruptly from the high level associated with massive dissolution inside the pits. More exactly, E_R was considered to be the potential at which the measured current density decreases below 0.2 mA cm^{-2} (on the backward scan).

Representative polarization curves for the five different Zr–Cu-based BMGs in 0.01 M Na_2SO_4 + 0.1 M NaCl are shown in Fig. 1. All alloys exhibit very low corrosion current density values below 10^{-3} mA cm^{-2} and

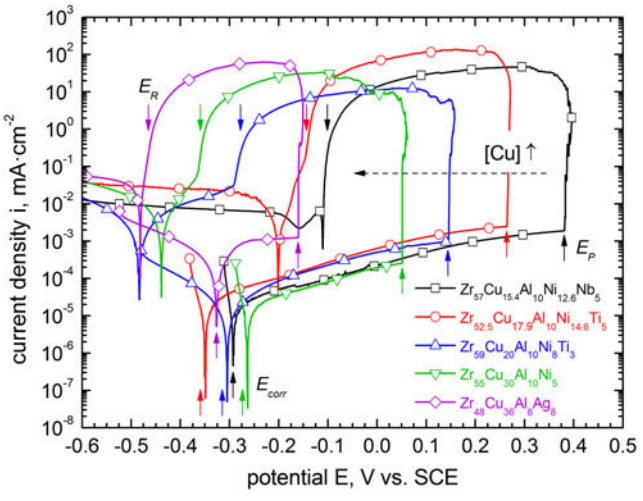

FIG. 1. Representative linear anodic polarization curves of Zr–Cu-based BMGs in 0.01 M Na_2SO_4 + 0.1 M NaCl solution (scan rate 0.5 mV s^{-1}). Corrosion, pitting, and repassivation potentials (E_{corr}, E_P, and E_R) are indicated by small arrows. The dashed horizontal arrow indicates the tendency of decreasing E_P and E_R values with increasing Cu content of the bulk glassy alloy.

a tendency to transfer into a passive plateau at current density values in the range of 10^{-3} mA cm^{-2}. The corrosion current density values determined in this study are significantly lower than those observed in previous works, e.g., by about one order of magnitude compared to Gebert et al.[34] This is attributed to aging of the samples in this study (for 20 h), which is expected to yield more protective native surface oxide films than those on freshly polished samples.[34] The corrosion potential, E_{corr}, is rather similar for all alloys, i.e., about −0.3 V versus SCE. As shown in Fig. 2, there is no clear dependence of E_{corr} on alloy composition. Previous surface analytical studies revealed that surface films on Zr-based metallic glasses formed naturally in air or under electrolyte exposure consist mostly of Zr oxides and contain additionally small amounts of other valve metals (in their oxide states), e.g., Al, Nb, and Ti.[4,17–19,21,37] Accordingly, the similar E_{corr} values of the glassy alloys studied here are attributed to their similar surface chemistry, i.e., consisting mostly of Zr oxides. Upon further increase in the potential (see Fig. 1), a sudden rapid increase in the current by several orders of magnitude occurs at E_P for all alloys, corresponding to the onset of stable pit growth. The current density (related to the geometric surface of the electrode) rapidly reaches the preset value of 1 mA cm^{-2} at which point the sweep direction is reversed. Still, the current density continues to increase up to values of 10–100 mA cm^{-2}, which are sustained as the potential is further decreased. Massive release of white corrosion products from pits was observed during the experiments. The white color of the corrosion products indicates the presence of large amounts of $ZrCl_4$ and/or CuCl. Upon further decrease of the polarization on the backward scan, repassivation of pits (or more generally said, cessation of pit growth) takes place at potentials E_R, which are significantly less noble than E_P. The high pitting current and the large hysteresis in the potential scan indicate poor repassivation ability for all five glassy alloys. In fact, as the measured anodic current in the backward scan at $E < E_R$ does not decrease back to the low values of the originally passive state, it is questionable whether true repassivation of pits takes place. Still, the very sharp decrease in current upon cessation of pit growth points to a repassivation process. Indeed, it appears that a low anodic current density corresponding to an entirely passive surface might be obscured by a superimposed high cathodic current. The responsible cathodic reaction(s) might be reduction of H^+ ions, of dissolved oxygen or/and of metallic or metal-containing complex ions, which were produced during the pitting process.[38] Reduction of H^+ ions is ruled out since the equilibrium potential of H^+/H_2 (−0.64 V versus SCE) is much lower than the corrosion potential of all alloys in the backward scan. Nevertheless, immediately after repassivation, the local level of acidity resulting from the pitting process might still be very high. Therefore, a small but probably negligible contribution of the hydrogen reduction reaction to the cathodic current is possible. Reduction of oxygen is expected to contribute to the observed cathodic current with only a small fraction due to its low concentration in the electrolyte (nonaerated conditions). Therefore, reduction of metallic or metal-containing complex ions produced during the pitting process is regarded as the main cathodic reaction in the backward scan. Finally, the relatively constant cathodic current density level (in the backward scan) suggests a mass-transport-limited reduction reaction.

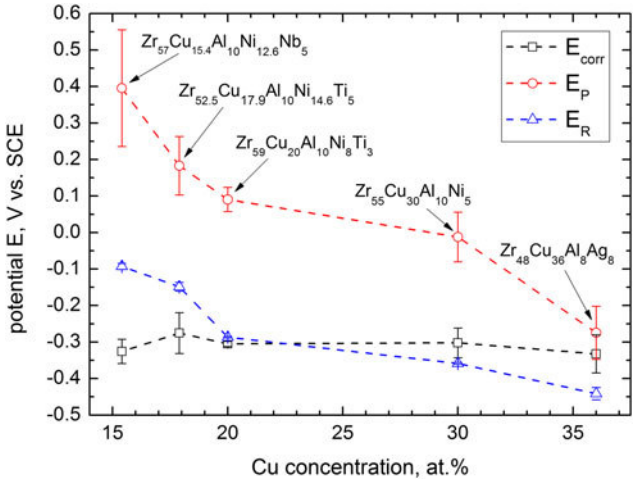

FIG. 2. Corrosion potential (E_{corr}), pitting potential (E_P), and repassivation potential (E_R) of five Zr–Cu-based BMGs in 0.01 M Na_2SO_4 + 0.1 M NaCl solution plotted against the Cu concentration in the alloys. The symbols represent mean values of five individual measurements. The error bars represent standard deviation.

As indicated in Fig. 1, both E_R and E_P decrease with increasing Cu concentration. Figure 2 shows a plot of several characteristic potentials derived from the potentiodynamic polarization experiments, i.e., E_{corr}, E_P, and E_R, against the Cu concentration for the five Zr–Cu-based BMGs studied here. E_{corr} is not significantly influenced by alloy composition. As explained earlier (see second paragraph of this section), the similar E_{corr} values are attributed to the similar surface chemistry of all studied glassy alloys, i.e., consisting mostly of Zr oxides. However, both E_R and E_P appear to decrease almost linearly with the Cu content. Additionally, the difference $E_P - E_R$ also tends to decrease with increasing Cu content. It is highest (0.49 V) for the glassy alloy with the lowest Cu content ($Zr_{57}Cu_{15.4}Al_{10}Ni_{12.6}Nb_5$) and lowest (0.17 V) for the glassy alloy with the highest Cu content ($Zr_{48}Cu_{36}Al_8Ag_8$). E_P shows the typical wide experimental scatter, in the order of hundreds of mV.[39] Onset of pitting strongly depends on the nature and number of weak points at the glassy sample cross-section

(inclusions, mechanical defects), which locally weaken the passive film and which are different for each new repeated experiment. On the contrary, E_R is very reproducible for all alloys, i.e., it has a standard deviation of 2–17 mV. While all five investigated alloys have a E_P higher than E_{corr}, only the $Zr_{57}Cu_{15.4}Al_{10}Ni_{12.6}Nb_5$ (Vit 106) and $Zr_{52.5}Cu_{17.9}Al_{10}Ni_{14.6}Ti_5$ (Vit 105) alloys also have a E_R significantly higher than E_{corr} suggesting that pitting is very unlikely to occur for those two glassy alloys at free corrosion conditions in a neutral 0.01 M Na_2SO_4 + 0.1 M NaCl solution.

In summary, all the Zr–Cu-based BMGs studied here have a relatively high pitting susceptibility and poor repassivation ability. Both the pitting resistance and the repassivation ability decrease significantly with increasing Cu content in the investigated interval of 15.4–36 at.%. Nevertheless, the effect of other alloying elements must also be considered as will be discussed later.

B. Pit morphology and chemistry

To better understand differences in the pitting process among the various Zr–Cu-based BMGs investigated here, further microscopic and chemical analyses were carried out. More specifically, SEM and EDX investigations were conducted on alloy sample cross-sections at an early stage of stable pit growth (when polarization was interrupted at i = 1 mA cm^{-2}) and after repassivation (at i = 0.2 μA cm^{-2} in the backward scan). To prevent alteration of pits, the samples were extracted from the test electrolyte immediately (within a few seconds) after the polarization was interrupted.

On all glassy alloy surfaces early pits exhibit similar features indicating that initially pit growth is similar in all cases. The early pits are hemispherical with smooth walls suggesting mass transport limited growth.[39] Often pits are initially covered by a layer, which is then rapidly damaged, as shown exemplarily in the SEM image in Fig. 3. EDX mapping revealed that the pit cover layer is enriched in Cu, O, and Cl as compared to the nonaffected region around the pit implying that Cu is related to the pitting mechanism. The observed enrichment of Cu, O, and Cl might correspond to compounds of those elements such as Cu_2O and CuCl. This confirms observations by Green et al.[19] and Paillier et al.[40]

Corresponding to the continued large current density level in the backward scan (Fig. 1), extensive pit growth takes place after reversing the polarization direction. After repassivation, a few tens of pits were observed on the surface of all alloys, some of which were larger than 100 μm. At this stage, the pits on all glassy alloys have similar morphological and compositional characteristics. Figure 4 shows such a large pit on the $Zr_{52.5}Cu_{17.9}Al_{10}Ni_{14.6}Ti_5$ bulk glassy alloy surface.

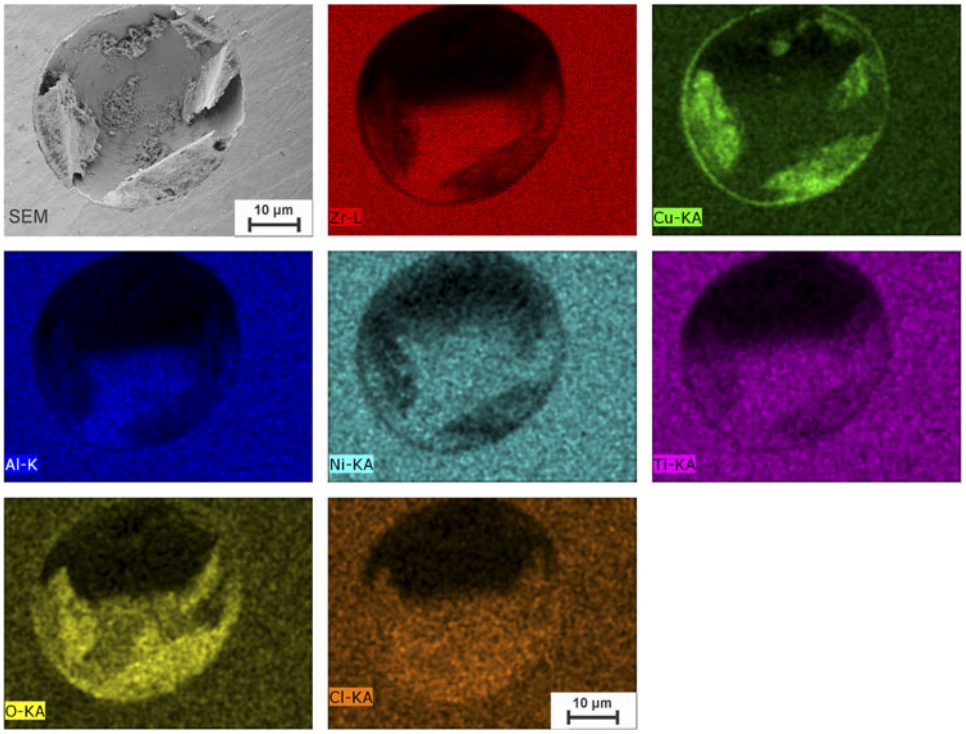

FIG. 3. SEM image and EDX mapping of an early state of a growing pit on the cross-section of a $Zr_{52.5}Cu_{17.9}Al_{10}Ni_{14.6}Ti_5$ bulk metallic sample glass (Vit 105). The pit was obtained by linear anodic polarization in 0.01 M Na_2SO_4 + 0.1 M NaCl solution up to the pitting potential E_P (polarization was interrupted at i = 1 mA cm^{-2}).

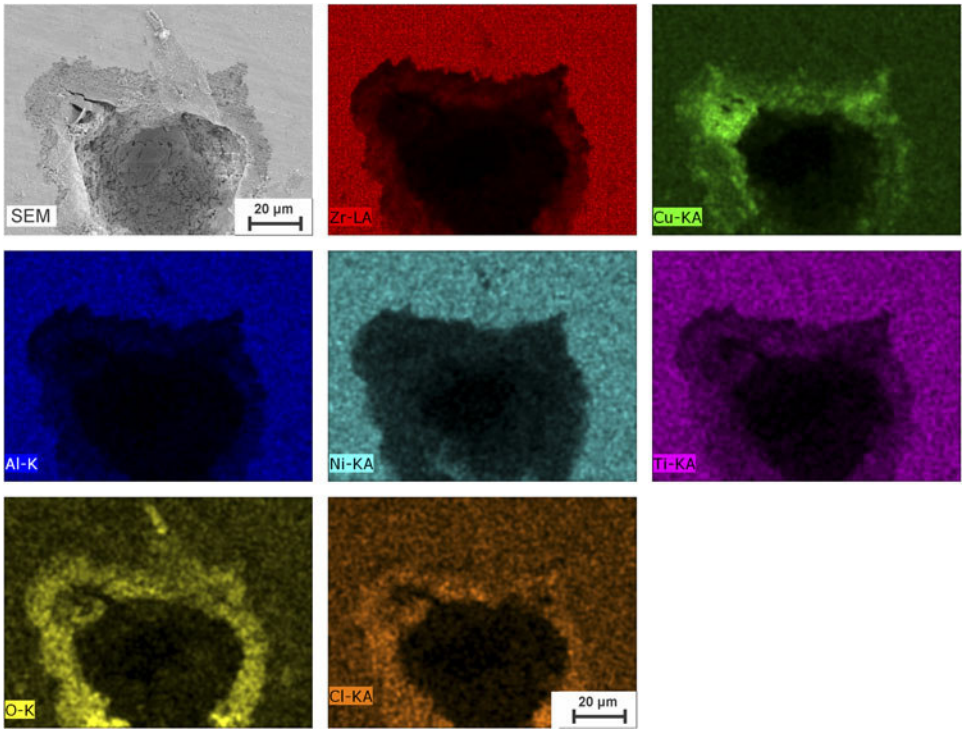

FIG. 4. SEM image and EDX mapping of a pitted area on the cross-section of a $Zr_{52.5}Cu_{17.9}Al_{10}Ni_{14.6}Ti_5$ bulk metallic glass (Vit 105) sample observed after extensive growth and repassivation. The pit was obtained by linear anodic polarization to the pitting potential E_P and subsequent reverse scanning to the repassivation potential E_R.

The pits are deep and have an irregular shape with an intricate growing front. The pit walls are not smooth as they were initially at E_P (see Fig. 3), but rather rough with pores and cracks. In some pits, the formerly smooth (electropolished) surface can still be recognized. The porous pit walls are 10–20 µm thick. EDX maps as those in Fig. 4 reveal that at the sample surface the porous walls are depleted of valve metals and of Ni, and enriched in Cu, O, and Cl.

In summary, the evolution of the pit morphology and the associated microchemical changes in typical Zr–Cu-based BMGs are rather similar. Initially, pits are hemispherical and grow under a cover, which is then rapidly damaged as the pit size increases. At a later stage, pits develop an irregular shape and a porous rim forms which is rich in Cu, O, and often Cl species.

IV. DISCUSSION

The data presented in Sec. III. A and III. B provide evidence of significant differences in the pitting resistance and repassivation ability of five typical Zr–Cu-based BMGs with various compositions. Both the pitting potential E_P and the repassivation potential E_R of those Zr–Cu-based BMGs correlate with the Cu content in the range of 15.4–36 at.%. That means, the higher the Cu content, the lower the E_P and E_R. This correlation may suggest that Cu tends to increase the pitting susceptibility of Zr–Cu-based BMGs. Further proof is gained from the SEM and the EDX investigations revealing Cu species enrichment in the porous walls of well-developed pits.

A detrimental effect of Cu on the pitting corrosion of Cu-containing Zr-based metallic glasses (both "bulk glassy" and nonbulk only glassy) can be inferred also from previous works. Huang et al. found that increasing the Cu content by 5 at.% in the bulk glassy $Zr_{55-x}Cu_{30+x}Al_7Nb_5Pd_3$ alloy decreases its E_P in a phosphate-buffered saline solution by about 0.2 V.[6] Binary Zr–Cu metallic glasses with 40–60 at.% Cu have pitting potentials much lower than that of pure Zr.[7,41] Cu-containing glassy alloys $Zr_{58}Cu_{28}Al_{10}Ti_4$ and $Zr_{65}Cu_{7.5}Al_{7.5}Ni_{10}Pd_{10}$ have better glass-forming ability than Cu-free alloy $Zr_{55}Ti_{25}Ni_{20}$. However, the Cu-containing alloys exhibit pitting in the 0.5 M NaCl solution already at E_{corr}, while the Cu-free alloy does not suffer from pitting up to 1 V versus SCE in the same solution.[3] In the same solution, the glassy $Zr_{70}Cu_6Al_8Ni_{16}$ alloy has an E_P value which is more noble than that of glassy $Zr_{50}Cu_{40}Al_{10}$ by more than 0.4 V.[42] Replacing Cu by Ni in the bulk glassy alloy $Zr_{60}Cu_{25-x}Al_{15}Ni_x$ (x = 0, 15, 25) greatly enhances its glass-forming ability, but at the same time causes a significant increase in E_P of up to almost 0.4 V.[15]

The bulk glassy $Zr_{52.5}Cu_{17.9}Al_{10}Ni_{14.6}Ti_5$ alloy (Vit 105) has a significantly higher pitting resistance in NaCl solutions compared to two glassy alloys with higher Cu content, i.e., $Zr_{50}Cu_{40}Al_{10}$ and $Zr_{50}Cu_{33}Al_{10}Pd_7$.[43] Interestingly, Cu was also found to deteriorate the oxidation resistance of Zr-based metallic glasses.[44] Although those previous works did not study systematic variations of the Cu concentration, they nevertheless provide some hints that Cu may have a strong influence on the pitting susceptibility of Zr–Cu-based metallic glasses. It must be noted that the glass-forming ability of multicomponent Zr–Cu-based alloys is quite sensitive to variations of alloying element concentration. Significant variation of the Cu content in a compositionally optimized multicomponent BMG causes a reduction of the glass-forming ability and partial crystallization, which is principally known to induce local corrosion phenomena. Therefore, those previous comparative corrosion studies included typically both bulk and nonbulk glassy alloys. The present comparative study focuses only on established monolithic Zr–Cu-based BMGs with maximum glass-forming ability for the respective multicomponent systems.[1,29]

Similar results of microscopic and chemical analyses of pits, e.g., by SEM and EDX, were reported for a variety of Zr–Cu-based metallic glasses. Typically, as observed also in this work, pits grow initially under a thin cover and are hemispherical in shape.[4,7,40] The occlusion of pits' interior by a cover may enhance the stability of the pitting process by maintaining an aggressive pit environment.[39,45] We noted that the cover consists of Cu compound(s) implying that Cu plays a decisive role in the initial stage of pit growth. The hemispherical shape and the occluded condition suggest that early pits on Zr–Cu-based metallic glasses grow under mass transport control.[39,45–47] If the pits are allowed to grow further, either by simply keeping the sample immersed,[9,40,42] or by increasing[3,4,7,19,48,49] or decreasing polarization (performed in this work) once E_P is reached, their morphology becomes more complex. They develop an irregular shape with deep holes and often a porous rim. In most of those previous studies as well as in the present one, the pits appeared to be rich in Cu, O, and often Cl indicating the presence of Cu oxide(s) and chloride(s). These results are in agreement with the generally accepted view that the initial local selective dissolution of Zr and other valve metal components leaves the surface locally (in the pit) rich in Cu species. It is further claimed that the Cu species in the enriched area react with chloride ions to form CuCl, which then in turn undergoes hydrolysis to form Cu_2O.[4,10,19,21,26–28] As a result, as demonstrated in this work, the Cu content in Zr–Cu-based BMGs (in the interval 15.4–36 at.%) plays an important role for their pitting behavior.

Within the set of Zr–Cu-based BMGs studied here, besides the content of Cu, the nature and concentration of other alloying elements also vary from alloy to alloy. Therefore, the difference in pitting resistance among the five glassy alloys cannot be attributed only to the different Cu contents. Other alloying elements may also play a significant role. The Al content is nearly similar in all alloys. While the base elements Zr and Ni have a certain susceptibility to pitting, Nb and Ti are known to generate extremely stable passive films in aqueous solutions that are particularly resistant to breakdown in the presence of chlorides. In consequence, the three alloys in this study containing Nb or Ti show higher E_P and E_R, which may be attributed to the low Cu content, but also to the presence of Nb or Ti. Indeed, previous works showed that additions of Nb or Ti to Zr-based BMGs cause an increase in E_P.[12,14,23,24] This improvement was attributed to the incorporation of Nb or Ti oxides into the Zr oxide rich passive film, which were assumed to hinder breakdown of the passive film.[13,22] In the presence of the chloride ion, Ag reacts with Cl^- to form various solid products and complex ions (e.g., $AgCl_{(s)}$ and $AgCl_2^-$ in neutral solutions).[50] It is therefore seen as detrimental for the pitting resistance. In the end, it is concluded that a combination of low Cu and high Nb or Ti contents is most beneficial for the pitting resistance of Zr–Cu-based BMGs. Therefore, the bulk glassy $Zr_{57}Cu_{15.4}Al_{10}Ni_{12.6}Nb_5$ (Vit 106) and $Zr_{52.5}Cu_{17.9}Al_{10}Ni_{14.6}Ti_5$ (Vit 105) alloys exhibit the highest corrosion stability and repassivation ability in this comparative study.

V. CONCLUSIONS

The pitting resistance and repassivation ability of Zr–Cu-based BMGs in chloride-containing neutral solution are limited. In a comparative study with five prominent strong bulk glass formers, both pitting and repassivation potential were found to decrease with increasing Cu content varying in the range of 15.4–36 at.%. A combination of low Cu and high Nb or Ti contents is most beneficial for a high pitting resistance and repassivation ability of those Zr–Cu-based BMGs. Conversely, high Cu and Ag contents are detrimental. Pit morphology is independent of composition: while initially hemispherical pits then develop an irregular shape and a porous rim rich in Cu, O, and often Cl species suggesting that Cu plays an important role in pit growth and repassivation.

According to these investigations, the bulk glassy $Zr_{57}Cu_{15.4}Al_{10}Ni_{12.6}Nb_5$ (Vit 106) and $Zr_{52.5}Cu_{17.9}Al_{10}Ni_{14.6}Ti_5$ (Vit 105) alloys represent a good target for further systematic fundamental studies on stress corrosion cracking, as they have suitable potential windows between the characteristic potentials (E_{corr}, E_P, and E_R) for stress corrosion cracking tests in chloride-containing environments.

Ultimately, $Zr_{52.5}Cu_{17.9}Al_{10}Ni_{14.6}Ti_5$ (Vit 105) is preferred as its pitting potential is less scattered than that of $Zr_{57}Cu_{15.4}Al_{10}Ni_{12.6}Nb_5$ (Vit 106).

ACKNOWLEDGMENTS

G.S. Frankel is acknowledged for fruitful discussions and motivation for this study. The authors are grateful to D. Beitelschmidt for fruitful discussions, to M. Johne and F. Mayr for electrochemical tests, and to M. Frey and S. Donath for sample preparation. Funding from the German Research Foundation (DFG) under project Ge1106/11 in the Priority Program SPP-1594 is gratefully acknowledged.

REFERENCES

1. C. Suryanarayana and A. Inoue: *Bulk Metallic Glasses* (CRC Press, Boca Raton, 2011).
2. A. Gebert, K. Mummert, J. Eckert, and L. Schultz: Electrochemical investigations on the bulk glass forming $Zr_{55}Cu_{30}Al_{10}Ni_5$ alloy. *Mater. Corros.* **48**, 293 (1997).
3. K. Mondal, B.S. Murty, and U.K. Chatterjee: Electrochemical behavior of multicomponent amorphous and nanocrystalline Zr-based alloys in different environments. *Corros. Sci.* **48**, 2212 (2006).
4. U. Kamachi Mudali, S. Baunack, J. Eckert, L. Schultz, and A. Gebert: Pitting corrosion of bulk glass-forming zirconium-based alloys. *J. Alloys Compd.* **377**, 290 (2004).
5. J.R. Scully, A. Gebert, and J. Payer: Corrosion and related mechanical properties of bulk metallic glasses. *J. Mater. Res.* **22**, 302 (2007).
6. L. Huang, Y. Yokoyama, W. Wu, P.K. Liaw, S.J. Pang, A. Inoue, T. Zhang, and W. He: Ni-free Zr-Cu-Al-Nb-Pd bulk metallic glasses with different Zr/Cu ratios for biomedical applications. *J. Biomed. Mater. Res. B. Appl. Biomater.* **100B**, 1472 (2012).
7. H.B. Lu, L.C. Zhang, A. Gebert, and L. Schultz: Pitting corrosion of Cu–Zr metallic glasses in hydrochloric acid solutions. *J. Alloys Compd.* **462**, 60 (2008).
8. A. Gebert, U. Kamachi Mudali, J. Eckert, and L. Schultz: In *Materials Research Society Symposium Proceedings* (Materials Research Society, Warrendale, PA, 2004), p. 369–379.
9. B.A. Green, R.V. Steward, I. Kim, C.K. Choi, P.K. Liaw, K.D. Kihm, and Y. Yokoyama: In situ observation of pitting corrosion of the $Zr_{50}Cu_{40}Al_{10}$ bulk metallic glass. *Intermetallics* **17**, 568 (2009).
10. W.H. Peter, R.A. Buchanan, C.T. Liu, P.K. Liaw, M.L. Morrison, J.A. Horton, C.A.J. Carmichael, and J.L. Wright: Localized corrosion behavior of a zirconium-based bulk metallic glass relative to its crystalline state. *Intermetallics* **10**, 1157 (2002).
11. M.L. Morrison, R.A. Buchanan, A. Peker, W.H. Peter, J.A. Horton, and P.K. Liaw: Cyclic-anodic-polarization studies of a $Zr_{41.2}Ti_{13.8}Ni_{10}Cu_{12.5}Be_{22.5}$ bulk metallic glass. *Intermetallics* **12**, 1177 (2004).
12. S.J. Pang, T. Zhang, H. Kimura, K. Asami, and A. Inoue: Corrosion behavior of Zr-(Nb-)Al-Ni-Cu glassy alloys. *Mater. Trans. JIM* **41**, 1490 (2000).
13. S.J. Pang, T. Zhang, K. Asami, and A. Inoue: Formation, corrosion behavior, and mechanical properties of bulk glassy Zr–Al–Co–Nb alloys. *J. Mater. Res.* **18**, 1652 (2003).
14. V.R. Raju, U. Kühn, U. Wolff, F. Schneider, J. Eckert, R. Reiche, and A. Gebert: Corrosion behaviour of Zr-based bulk glass-forming alloys containing Nb or Ti. *Mater. Lett.* **57**, 173 (2002).
15. Y.H. Li, W. Zhang, C. Dong, J.B. Qiang, M. Fukuhara, A. Makino, and A. Inoue: Effects of Ni addition on the glass-forming ability, mechanical properties and corrosion resistance of Zr–Cu–Al bulk metallic glasses. *Mater. Sci. Eng., A* **528**, 8551 (2011).
16. Z. Liu, L. Huang, W. Wu, X. Luo, M. Shi, P.K. Liaw, W. He, and T. Zhang: Novel low Cu content and Ni-free Zr-based bulk metallic glasses for biomedical applications. *J. Non-Cryst. Solids* **363**, 1 (2013).
17. A. Gebert, K. Buchholz, A. Leonhard, K. Mummert, J. Eckert, and L. Schultz: Investigations on the electrochemical behaviour of Zr-based bulk metallic glasses. *Mater. Sci. Eng., A* **267**, 294 (1999).
18. S. Baunack, U. Kamachi Mudali, and A. Gebert: Characterization of oxide layers on amorphous Zr-based alloys by Auger electron spectroscopy with sputter depth profiling. *Appl. Surf. Sci.* **252**, 162 (2005).
19. B.A. Green, H.M. Meyer, R.S. Benson, Y. Yokoyama, P.K. Liaw, and C.T. Liu: A study of the corrosion behaviour of $Zr_{50}Cu_{(40-X)}Al_{10}Pd_X$ bulk metallic glasses with scanning Auger microanalysis. *Corros. Sci.* **50**, 1825 (2008).
20. S. Hiromoto, A.P. Tsai, M. Sumita, and T. Hanawa: Effect of chloride ion on the anodic polarization behavior of the $Zr_{65}Al_{7.5}Ni_{10}Cu_{17.5}$ amorphous alloy in phosphate buffered solution. *Corros. Sci.* **42**, 1651 (2000).
21. N. Homazava, A. Shkabko, D. Logvinovich, U. Krähenbühl, and A. Ulrich: Element-specific in situ corrosion behavior of Zr–Cu–Ni–Al–Nb bulk metallic glass in acidic media studied using a novel microcapillary flow injection inductively coupled plasma mass spectrometry technique. *Intermetallics* **16**, 1066 (2008).
22. X.P. Nie, X.M. Xu, Q.K. Jiang, L.Y. Chen, Y. Xu, Y.Z. Fang, G.Q. Xie, M.F. Luo, F.M. Wu, X.D. Wang, Q.P. Cao, and J.Z. Jiang: Effect of microalloying of Nb on corrosion resistance and thermal stability of ZrCu-based bulk metallic glasses. *J. Non-Cryst. Solids* **355**, 203 (2009).
23. L. Liu, C.L. Qiu, M. Sun, Q. Chen, K.C. Chan, and G.K.H. Pang: Improvements in the plasticity and biocompatibility of Zr–Cu–Ni–Al bulk metallic glass by the microalloying of Nb. *Mater. Sci. Eng., A* **449–451**, 193 (2007).
24. K. Asami, H. Habazaki, A. Inoue, and K. Hashimoto: Recent development of highly corrosion resistant bulk glassy alloys. *Mater. Sci. Forum* **502**, 225 (2005).
25. A. Gebert, P.F. Gostin, M. Uhlemann, J. Eckert, and L. Schultz: Interactions between mechanically generated defects and corrosion phenomena of Zr-based bulk metallic glasses. *Acta Mater.* **60**, 2300 (2012).
26. H. Tanimoto, Y. Soga, Y. Takayanagi, and H. Mizubayashi: Dissolved-oxygen-induced intensive pitting corrosion of amorphous ZrCu alloys in thin NaCl solutions. *Mater. Trans.* **52**, 1402 (2011).
27. A. Gebert, U. Kuehn, S. Baunack, N. Mattern, and L. Schultz: Pitting corrosion of zirconium-based bulk glass-matrix composites. *Mater. Sci. Eng., A* **415**, 242 (2006).
28. V. Schroeder, C.J. Gilbert, and R.O. Ritchie: Comparison of the corrosion behaviour of a bulk amorphous metal, $Zr_{41.2}Ti_{13.8}Cu_{12.5}Ni_{10}Be_{22.5}$, with its crystallized form. *Scr. Mater.* **38**, 1481 (1998).
29. Z. Long, H. Wei, Y. Ding, P. Zhang, G. Xie, and A. Inoue: A new criterion for predicting the glass-forming ability of bulk metallic glasses. *J. Alloys Compd.* **475**, 207 (2009).
30. J.J. Kruzic: Understanding the problem of fatigue in bulk metallic glasses. *Metall. Mater. Trans. A* **42**, 1516 (2010).
31. A. Kawashima, Y. Yokoyama, and A. Inoue: Zr-based bulk glassy alloy with improved resistance to stress corrosion cracking in sodium chloride solutions. *Corros. Sci.* **52**, 2950 (2010).

32. V. Schroeder, C.J. Gilbert, and R.O. Ritchie: Effect of aqueous environment on fatigue-crack propagation behavior in a Zr-based bulk amorphous metal. *Scr. Mater.* **40**, 1057 (1999).
33. M.L. Morrison, R. Buchanan, P. Liaw, B.A. Green, G. Wang, C. Liu, and J.A. Horton: Corrosion–fatigue studies of the Zr-based Vitreloy 105 bulk metallic glass. *Mater. Sci. Eng., A* **467**, 198 (2007).
34. A. Gebert, P.F. Gostin, and L. Schultz: Effect of surface finishing of a Zr-based bulk metallic glass on its corrosion behaviour. *Corros. Sci.* **52**, 1711 (2010).
35. ASTM: *Standard Test Methods for Pitting and Crevice Corrosion Resistance of Stainless Steels and Related Alloys by Use of Ferric Chloride Solution* (ASTM International, West Conshohocken, PA 2000).
36. G.S. Frankel, J.R. Scully, and C. Jahnes: Repassivation of pits in aluminum thin films. *J. Electrochem. Soc.* **143**, 1834 (1996).
37. B. Vishwanadh, G.J. Abraham, J.S. Neogy, R.S. Dutta, and G.K. Dey: Effect of structural defects, surface irregularities, and quenched-in defects on corrosion of Zr-based metallic glasses. *Metall. Mater. Trans. A* **40A**, 1131 (2009).
38. Y.H. Kim and G.S. Frankel: Effect of noble element alloying on passivity and passivity breakdown of Ni. *J. Electrochem. Soc.* **154**, C36 (2007).
39. G.S. Frankel: Pitting corrosion of metals. A review of the critical factors. *J. Electrochem. Soc.* **145**, 2186 (1998).
40. J. Paillier, C. Mickel, P.F. Gostin, and A. Gebert: Characterization of corrosion phenomena of Zr–Ti–Cu–Al–Ni metallic glass by SEM and TEM. *Mater. Charact.* **61**, 1000 (2010).
41. H. Bala and S. Szymura: Acid corrosion of amorphous and crystalline Cu-Zr alloys. *Appl. Surf. Sci.* **35**, 41 (1988).
42. A. Kawashima, K. Ohmura, Y. Yokoyama, and A. Inoue: The corrosion behaviour of Zr-based bulk metallic glasses in 0.5M NaCl solution. *Corros. Sci.* **53**, 2778 (2011).
43. B.A. Green: Localized corrosion behaviour of Zr-based bulk metallic glasses in neutral NaCl electrolytes. Doctoral Dissertation, The University of Tennessee, Knoxville, TN, 2008.
44. U. Köster and Triwikantoro: Oxidation of amorphous and nanocrystalline Zr-Cu-Ni-Al alloys. *Mater. Sci. Forum* **360–362**, 29 (2001).
45. H-H. Strehblow: In *Corrosion Mechanisms in Theory and Practice*, P. Marcus ed.; Marcel Dekker, Inc.: New York, Basel, 2002; pp. 243–285.
46. N.J. Laycock and R.C. Newman: Localised dissolution kinetics, salt films and pitting potentials. *Corros. Sci.* **39**, 1771 (1997).
47. N. Sato: The stability of localized corrosion. *Corros. Sci.* **37**, 1947 (1995).
48. A. Tauseef, N.H. Tariq, J.I. Akhter, B.A. Hasan, and M. Mehmood: Corrosion behavior of Zr–Cu–Ni–Al bulk metallic glasses in chloride medium. *J. Alloys Compd.* **489**, 596 (2010).
49. A. Gebert, F. Gostin, U. Kühn, and L. Schultz: Corrosion of a Zr-based bulk metallic glass with different surface finishing states. *ECS Trans.* **16**, 1 (2009).
50. W.T. Thompson, M.H. Kaye, C.W. Bale, and A.D. Pelton: In *Uhlig's Corrosion Handbook*, R.W. Revie ed. (John Wiley & Sons, Inc., New York, NY, 2000); pp. 125–136.